Struct Multidisc Optim 22, 284–294

Convex analysis for topology optimization of compliant mechanisms

G.K. Lau, H. Du and M.K. Lim

Abstract This paper analyses the convexity of the problem formulations for topological optimization of compliant mechanisms. In this context, a ground structure is assumed to consist of membranes with variable thickness or trusses with variable cross-sectional area. It is proven that the objective function of maximum mechanical or geometrical advantage may not be convex even though the constraints for the problem formulations give rise to a convex set. The constraints include volumetric constraint and a bound on input displacement. The nonconvex objective functions are shown analytically with two examples using truss elements. Also, it is illustrated numerically with an example using bilinear quadrilateral elements. It is concluded that nonconvex objective functions also attribute to difficulties in arriving at the globally optimal topology of compliant mechanisms, in addition to the number of design variables and constraints. As the problem is more complicated, the solution of the problem requires robust and reliable optimization techniques.

Key words convex analysis, topology optimization, compliant mechanism, maximum flexibility, nonconvex property

1 Introduction

Systematic synthesis methods for compliant mechanisms has been developed using topology optimization. The idea of automating design by using topology optimization consists of determining the shape and connectivity of compliant mechanisms using raster representation. Instead of predetermining the number of links and the location of flexural joints as type synthesis does, topology optimization automatically suggests raster-like or bit-wise images of feasible design for planar compliant mechanisms provided the design domain, boundary conditions and functional specifications are prescribed. To realize such a design methodology, formal techniques of structural optimization are adopted but the design goals are modified specifically to suit the functional requirement of compliant mechanisms. The design problem can be posed as a problem of material distribution such that the objective function is extremized while constraints are satisfied. The optimal shape or topology is represented by distribution of point-wise solid belonging to the domain Ω^s over the reference design domain Ω, which is discretized into a finite number of N elements. A solid element is characterized by the constant elasticity tensor $\mathbf{E}^0_{ijk}$ while a void element does not exhibit rigidity. Mathematically, the problem is thus to determine the optimal $\mathbf{E}_{ijk\ell}(x)$ which varies over the design domain Ω (Bendsøe 1989) and takes the form

$$\mathbf{E}_{ijk\ell}(x) = \chi(x)\mathbf{E}^0_{ijk\ell}\,, \tag{1}$$

where $\chi(x)$ is an indicator function that defines the distribution of material

$$\chi(x) = \begin{cases} 1 & \text{if } x \in \Omega^s\,, \\ 0 & \text{if } x \in \Omega \setminus \Omega^s\,. \end{cases} \tag{2}$$

To obtain a useful and feasible design based on a raster-like topological image, the objective function must be properly formulated. It is generally known that the major function of compliant mechanisms is to transfer work from input port to output port. Hence, most objective functions are formulated in terms of input and output displacements. Researchers in Michigan and Pennsylvania (Ananthasuresh *et al.* 1994; Frecker *et al.* 1997, 1999; Nishiwaki *et al.* 1998; Saxena and Ananthasuresh 1998) used the notion of mutual potential energy (MPE), which is equivalent to output displacement, and strain energy (SE). They formulated multicriteria in the form of weighted sum of MPE and SE, the ratio of MPE to SE, and the power ratio of MPE to SE. Researchers in Den-

Received January 27, 2000
Revised manuscript received August 8, 2000

G.K. Lau, H. Du and M.K. Lim

School of Mechanical and Production Engineering, Nanyang Technological University, Nanyang Avenue, Singapore 639798
e-mail: mhdu@ntu.edu.sg

mark (Sigmund 1997; Larsen *et al.* 1997) adopted different, kinematic approaches. They formulated the problem with maximum mechanical advantage, and minimum errors in obtaining prescribed geometrical and mechanical advantages.

Despite the success in obtaining some feasible designs, the solution of the compliant mechanism problem is generally more difficult than that of the minimum compliance problem for structures. In early work on topology optimization of compliant mechanisms, Ananthasuresh (1994) used optimal criteria to find optimal topologies. But the results obtained appear rather stiff and unlike flexible mechanisms. When multicriteria of higher complexity are involved, Frecker *et al.* (1997), Nishiwaki *et al.* (1998) found that it is difficult to develop an updating scheme and thus resorted to sequential linear programming. Later, Saxena and Ananthasuresh (1998) pursued an updating scheme that combines a resizing scheme and line-search at each iteration to ensure arrival at the minimum objective function. On the other hand, Sigmund (1997, 1998) successfully used sequential linear programming and the method of moving asymptotes to solve compliant mechanism problems for linear static and coupled-field response. In view of the higher complexity of the compliant mechanism problem, the solution of the problem generally requires robust and reliable optimization techniques.

Besides the number of constraints and design variables, the difficulty in synthesizing compliant mechanisms is mostly attributed to the nonlinear objective function. Saxena and Ananthasuresh (1998) demonstrated the nonconvexity and nonuniqueness of multicriteria using the examples of a beam and a compliant inverter. Using multicriteria as the objective function and the ground structure of a truss, Frecker *et al.* (1999) noted that even though MPE and SE are individually convex, the ratio of MPE to SE is not necessarily convex. However, the convexity for the problem formulations of maximum mechanical or geometrical advantages (Sigmund 1997; Lau *et al.* 1999) has yet to be analysed. Hence, this paper attempts to address their convexity and provide additional insight into the compliant mechanism problem. The nature of the problem formulation is expected to account for the difficulty in obtaining a solution.

2 Problem formulation for compliant mechanism design

To solve for the topology of compliant mechanisms using mathematical programming for continuous variables, the discrete design set in (2) is relaxed with a continuous design set of variable thickness, $t(x) \in (0, 1]$. In numerical implementation, the continuous design domain Ω is discretized into N finite elements. It is assumed that the continuum is made of a plane-stress membrane, whose material matrix $\mathbf{C}$ is given by

$$\mathbf{C} = \frac{E}{1-\nu^2}\begin{bmatrix} 1 & \nu & 0 \\ \nu & 1 & 0 \\ 0 & 0 & \frac{1-\nu}{2} \end{bmatrix}, \tag{3}$$

in which E is Young's modulus of the material used, ν is Poisson's ratio.

Hence, total volume can be written as

$$V(\mathbf{t}) = \int_{\Omega} t(x)\,\mathrm{d}\Omega = \sum_{i=1}^{N} t_i\,\mathrm{d}\Omega_i\,, \tag{4}$$

where $t(x)$ is a thickness function varying over the design domain Ω and is approximated by a vector $\mathbf{t}$ whose component t_i is constant over an element domain $\mathrm{d}\Omega_i$.

On the other hand, the stiffness matrix $\mathbf{K}(t)$ can be written as

$$\mathbf{K}(\mathbf{t}) = \sum_{i=1}^{N} t_i \mathbf{K}_i\,, \tag{5}$$

in which $\mathbf{K}_i$ denotes a constant element stiffness matrix on global level and per unit thickness.

Similarly, if the continuum is assumed to be a discrete truss, (4) and (5) are still valid. But t_i denotes the cross-sectional area of the truss and the material matrix $\mathbf{C}$ is a constant given by

$$\mathbf{C} = E\,. \tag{6}$$

Based on (3)–(6) and according to Lau *et al.* (1999), one can state the problem formulations as below, in which the mechanical advantage (MA) and geometrical advantages (GA) are posed as objective functions, respectively,

$$\max_{\mathbf{t}} \mathrm{MA}(\mathbf{t})\,,$$

subject to

$$u_{\mathrm{in}}(\mathbf{t}) < u^*_{\mathrm{in}}\,, \quad \frac{V(\mathbf{t})}{V_0} < V^*\,,$$

$$\mathbf{K}(\mathbf{t})\mathbf{u}(\mathbf{t}) = \mathbf{F}\,, \quad 0 < t_{\min} \le t_i \le t_{\max}\,, \tag{7}$$

and

$$\max_{\mathbf{t}} \mathrm{GA}(\mathbf{t})\,,$$

subject to

$$\frac{V(\mathbf{t})}{V_0} < V^*\,, \quad \mathbf{K}(\mathbf{t})\mathbf{u}(\mathbf{t}) = \mathbf{F}\,,$$

$$0 < t_{\min} \le t_i \le t_{\max}\,. \tag{8}$$

In the first formulation (7), MA denotes mechanical advantage of a resultant topology. If a spring model, as

shown in Fig. 1, is used to describe the interaction between a compliant mechanism and a workpiece, the output force is given by the force induced in the deflected spring. Hence, we have

$$\mathrm{MA} = \frac{k_s u_{\mathrm{out}}}{f_1}\,, \tag{9}$$

in which k_s is the spring constant for the workpiece, u_{out} is the output displacement, and f_1 is input force.

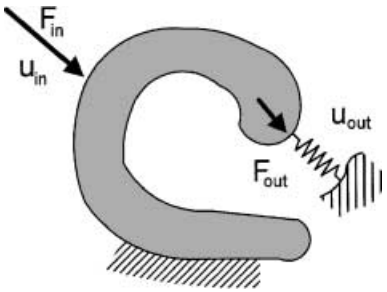

Fig. 1 Spring model

Stress and fatigue are of great concern in the design of compliant mechanisms. Stresses are induced whenever members are deflected and may cause premature failure of the mechanism. In addition, kinematic constraints also restrict flexural pivots from going through full rotation. Consequently, this leads to a bound on the input displacement in (7). The constraint serves to restrain the movement of input port and complement the objective function of MA, which does not restrain the input displacement.

Together with volume and side constraints, the constraint on input displacement is posed in a typical manner for constrained maximization. But equilibrium equations are solved separately using finite element analysis and are not dealt with directly in the optimization problem.

In the second formulation (8), GA denotes geometrical advantage of a resultant topology, and it is given by the ratio of output displacement to input displacement, i.e.

$$\mathrm{GA} = \frac{u_{\mathrm{out}}}{u_{\mathrm{in}}}\,. \tag{10}$$

When the objective function GA is maximized, the input displacement, u_{in}, which appears in the denominator of GA, is effectively minimized. Thus, without any additional input displacement constraint as in (7), the concerns on stress are still taken into account when using GA as the objective function.

3 Convex analysis for compliant mechanism problems

The convexity of the optimization problems (7) and (8) for compliant mechanism is closely related to minimum compliance problem. The objective functions of (7) and (8) are different from minimum compliance. But, the input displacement constraint in (7) is equivalent to a symmetric displacement constraint, which has been proven by Svanberg (1984) to be convex. This section attempts to study the convexity of constraints and subsequently that of the objective functions for (7) and (8). Before proceeding to study the convexity of constraints and objective functions, basic definitions for the optimum point, the positive definite matrix and convexity are reviewed. For more details on the fundamentals, readers are referred to books on nonlinear programming (Bertsekas 1995).

Definition 1. *A symmetric $n \times n$ matrix $\mathbf{A}$ is called positive definite if $\mathbf{x}^T\mathbf{A}\mathbf{x} > 0$ for all $\mathbf{x} \in \mathrm{Re}^n$, $\mathbf{x} \neq 0$. It is called non-negative definite or positive semidefinite if $\mathbf{x}^T\mathbf{A}\mathbf{x} \geq 0$ for all $\mathbf{x} \in \mathrm{Re}^n$. Generally, the notion of positive and negative definiteness applies exclusively to symmetric matrices.*

Definition 2. *A set C in Re^n is said to be convex if*

$$\mu\mathbf{X} + (1-\mu)\mathbf{Y} \in C\,, \tag{11}$$

for every $\mathbf{X}, \mathbf{Y} \in C$ and for every real number μ such that $0 < \mu < 1$.

Let V be a vector space of finite or infinite subscripts.

Lemma 1. *Let C_v, $v \in V$, be a collection of convex sets in Re^n. Then the intersection set*

$$C = \bigcap C_v = \{\mathbf{X} \in \mathrm{Re}^n | \mathbf{X} \in C_v \text{ for all } v \in V\} \tag{12}$$

is convex. If C is empty, then it is by definition convex.

Definition 3. *A real-value function φ, defined on a convex set C, is said to be convex over C if*

$$\varphi[\mu\mathbf{X} + (1-\mu)\mathbf{Y}] \leq \mu\varphi(\mathbf{X}) + (1-\mu)\varphi(\mathbf{Y})\,, \tag{13}$$

for every $\mathbf{X}, \mathbf{Y} \in C$ and for every μ such that $0 < \mu < 1$.

Lemma 2. *A linear function is convex by definition of convexity.*

For twice continuously differentiable functions there is an alternative characterization of convexity.

Lemma 3. *Assume that the function φ has continuous second partial derivatives on a convex set C in Re^n. Then φ is convex over C if and only if the Hessian matrix $\nabla^2\varphi(\mathbf{X})$ of φ is positive semi-definite throughout C, i.e. if and only if*

$$\mathbf{h}^T\nabla^2\varphi(\mathbf{X})\mathbf{h} = \sum\sum \frac{\partial^2\varphi}{\partial X_i \partial X_j} h_i h_j \geq 0\,, \tag{14}$$

for all $\mathbf{X} \in C$ and for every vector $\mathbf{h} \in \mathrm{Re}^n$.

Definition 4. *To simplify the optimization problems (7) and (8) for compliant mechanism design, we assume that single input and single output are dealt with. The directions of input and output motions are limited to orthogonal direction as the major degree of freedom used in the two-dimensional design domain. Hence, the design domain is only subject to a load vector* $\mathbf{p}$*, which is a vector having a nonzero element in row* i*,*

$$\mathbf{p} = f_1 \mathbf{e}_i \,. \tag{15}$$

On the other hand, the displacement vector for (8) and (9) can be solved by

$$\mathbf{u} = \mathbf{K}^{-1}\mathbf{p} \,, \tag{16}$$

where $\mathbf{K}$ *is a stiffness matrix, which is symmetric positive definite and linearly varying with respect to design variable,* t_i*, which is either the thickness of the membrane or the cross-sectional area. By Lemma 2, the inverse matrix of* $\mathbf{K}$*, i.e.* K^{-1}*, is also positive definite.*

Let $\mathbf{q}$ be a unit vector that specifies the degree of freedom for output displacement such that

$$\mathbf{q} = \mathbf{e}_j \,. \tag{17}$$

Using (15)–(17), the input and output displacements can be expressed as

$$u_{\text{in}} = \mathbf{e}_i^T \mathbf{u} = \frac{\mathbf{p}^T \mathbf{u}}{\|\mathbf{p}\|} = \frac{\mathbf{p}^T \mathbf{K}^{-1} \mathbf{p}}{\|\mathbf{p}\|} \,, \tag{18}$$

$$u_{\text{out}} = \mathbf{e}_j^T \mathbf{u} = \mathbf{q}^T \mathbf{u} = \mathbf{q}^T \mathbf{K}^{-1} \mathbf{p} \,. \tag{19}$$

Proposition 1. *The intersection of volume constraint and input displacement constraint gives rise to a convex feasible set.*

Proof. As the volume constraint, i.e.

$$\frac{V(\mathbf{t})}{V_0} < V^* \,, \tag{20}$$

is a linear function of thickness t_i, it is convex following from Lemma 3.

Similar to the symmetric displacement constraint (Svanberg 1984), the input displacement constraint can be proven convex. For completeness, the proof is repeated here.

From (7), the input displacement constraint is

$$u_{\text{in}} \le u^* \,. \tag{21}$$

Taking the derivative of $\mathbf{K}\mathbf{K}^{-1} = \mathbf{I}$ with respect to t_i, we have

$$\frac{\partial \mathbf{K}^{-1}}{\partial t_i} = -\mathbf{K}^{-1} \frac{\partial \mathbf{K}^{-1}}{\partial t_i} \mathbf{K}^{-1} \,. \tag{22}$$

Differentiating input displacement in (18) with respect to t_i and substituting (22), we have

$$\frac{\partial u_{\text{in}}}{\partial t_i} = -\mathbf{p}^T \mathbf{K}^{-1} \frac{\partial \mathbf{K}}{\partial t_i} \mathbf{K}^{-1} \frac{\mathbf{p}}{\|\mathbf{p}\|} \,. \tag{23}$$

Differentiating (23) with respect to t_j, we have

$$\frac{\partial^2 u_{\text{in}}}{\partial t_i \partial t_j} = \frac{1}{\|\mathbf{p}\|} \left[\mathbf{p}^T \mathbf{K}^{-1} \frac{\partial \mathbf{K}}{\partial t_j} \mathbf{K}^{-1} \frac{\partial \mathbf{K}}{\partial t_i} \mathbf{K}^{-1} \mathbf{p} + \right.$$

$$\left. \mathbf{p}^T \mathbf{K}^{-1} \frac{\partial \mathbf{K}}{\partial t_i} \mathbf{K}^{-1} \frac{\partial \mathbf{K}}{\partial t_j} \mathbf{K}^{-1} \mathbf{p} \right] . \tag{24}$$

One can prove the convexity of the input displacement constraint by checking the positive definiteness of the Hessian matrix of u_{in} as follows. Let $\mathbf{h} \in \text{Re}^n$,

$$\mathbf{h}^T \nabla^2 u_{\text{in}} \mathbf{h} = \sum_i \sum_j \frac{\partial^2 u_{\text{in}}}{\partial t_i \partial t_j} h_i h_j =$$

$$\frac{1}{\|\mathbf{p}\|} \left[\mathbf{p}^T \mathbf{K}^{-1} h_j \frac{\partial \mathbf{K}}{\partial t_j} \mathbf{K}^{-1} h_i \frac{\partial \mathbf{K}}{\partial t_i} \mathbf{K}^{-1} \mathbf{p} + \right.$$

$$\left. \mathbf{p}^T \mathbf{K}^{-1} h_i \frac{\partial \mathbf{K}}{\partial t_i} \mathbf{K}^{-1} h_j \frac{\partial \mathbf{K}}{\partial t_j} \mathbf{K}^{-1} \mathbf{p} \right] . \tag{25}$$

With $\mathbf{H} = \sum_i h_i (\partial \mathbf{K} / \partial t_i)$, which is symmetric, (25) can be reduced to the following:

$$\mathbf{h}^T \nabla^2 u_{\text{in}} \mathbf{h} = \frac{2}{\|\mathbf{p}\|} \mathbf{p}^T \mathbf{K}^{-1} \mathbf{H} \mathbf{K}^{-1} \mathbf{H} \mathbf{K}^{-1} \mathbf{p} =$$

$$\frac{2}{f_1} (\mathbf{H}\mathbf{K}^{-1}\mathbf{p})^T \mathbf{K}^{-1} (\mathbf{H}\mathbf{K}^{-1}\mathbf{p}) \ge 0 \,, \tag{26}$$

because $\mathbf{K}^{-1}$ is positive definite. Since $\mathbf{h}^T \nabla^2 u_{\text{in}} \mathbf{h} \ge 0$ for every $\mathbf{h} \in \text{Re}^n$ and $\mathbf{t} \in C$, it follows from Lemma 3 that (21) is convex. Since both constraints (20) and (21) are convex, it follows from Lemma 1 that the intersection of two convex sets gives rise to a convex set.

Proposition 2. *The objective function of maximum mechanical advantage in (7) may not be convex.*

Proposition 3. *The objective function of maximum geometrical advantage in (8) may not be convex.*

By presenting examples of nonconvex objective functions, propositions 2 and 3 can be proven. The first example deals with two-member trusses while the second example deals with six-member trusses.

3.1 Example 1

This example uses a simple ground structure, having two degrees of freedom and consisting of two-member trusses, whose areas A_1 and A_2 are to be determined so that mechanical or geometrical advantages at output port are maximized for the given input force P. Employing the spring model, an additional spring of stiffness k_s is to be attached between output port and ground. Hence, the structure has two trusses of variable area and a spring of fixed stiffness as shown in Fig. 2.

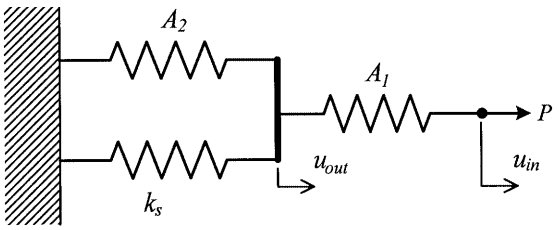

Fig. 2 Ground structure for example 1

After simple operations, the input and output displacements are derived as below,

$$u_{\text{in}} = \frac{k_1 + k_2 + k_s}{k_1(k_2 + k_s)} P \,, \tag{27}$$

$$u_{\text{out}} = \frac{P}{k_2 + k_s} \,, \tag{28}$$

where $k_1 = A_1 E/\ell$, $k_2 = A_2 E/\ell$.

Hence,

$$MA = \frac{k_s u_{\text{out}}}{P} = \frac{k_s}{k_2 + k_s} \,, \tag{29}$$

$$GA = \frac{u_{\text{out}}}{u_{\text{in}}} = \frac{k_1}{k_1 + k_2 + k_s} \,. \tag{30}$$

Performing partial differentiation, the Hessian of MA and GA is derived as

$$\nabla^2 MA = \begin{bmatrix} 0 & 0 \\ 0 & \frac{2k_s}{(k_2+k_s)^3} \end{bmatrix} \,, \tag{31}$$

$$\nabla^2 GA = \begin{bmatrix} -2(k_2 + k_s) & k_1 - k_2 - k_s \\ k_1 - k_2 - k_s & 2k_1 \end{bmatrix} \,. \tag{32}$$

To solve (7) as a minimization problem, the objective function is set to be $\varphi_1 = -MA$. Let $\mathbf{h} = (h_1, h_2)^T \in \mathrm{Re}^n$, the quadratic form on the Hessian of objective function φ_1 is found to be negative as

$$\mathbf{h}^T(\nabla^2 \varphi_1)\mathbf{h} = -\mathbf{h}^T(\nabla^2 MA)\mathbf{h} = -\frac{2k_s h_2^2}{(k_2 + k_s)^3} < 0 \,, \tag{33}$$

where k_s and k_2 are positive. This example shows that φ_1 is concave but not convex. Thus, Proposition 2 is proven.

Similarly, (8) can be solved as a minimization problem using an objective function $\varphi_2 = -GA$. The quadratic form of the Hessian of objective function φ_2 is

$$\mathbf{h}^T(\nabla^2 \varphi_2)\mathbf{h} = -\mathbf{h}^T(\nabla^2 GA)\mathbf{h} =$$

$$\frac{2(k_2 + k_s)h_1^2 - 2(k_1 - k_2 - k_s)h_1 h_2 - 2k_1 h_2^2}{(k_1 + k_2 + k_s)^3} \,. \tag{34}$$

At $\mathbf{h} = (1, 0)^T$,

$$\mathbf{h}^T(\nabla^2 \varphi_2)\mathbf{h} = \frac{2(k_2 + k_s)h_1^2}{(k_1 + k_2 + k_s)^3} > 0 \,.$$

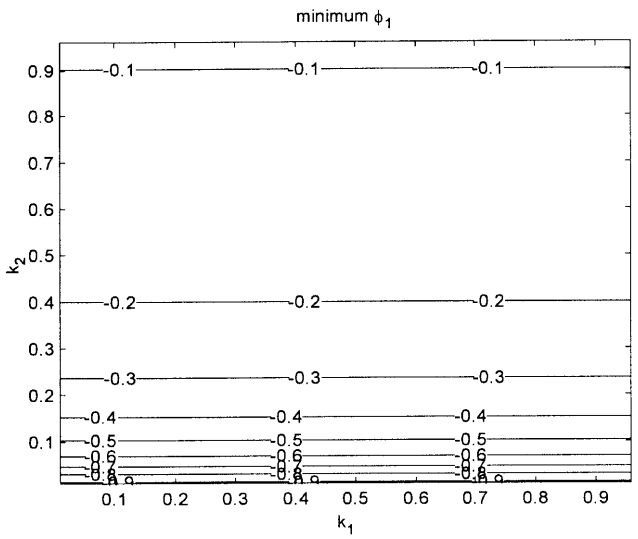

Fig. 3 Contour plot for φ_1

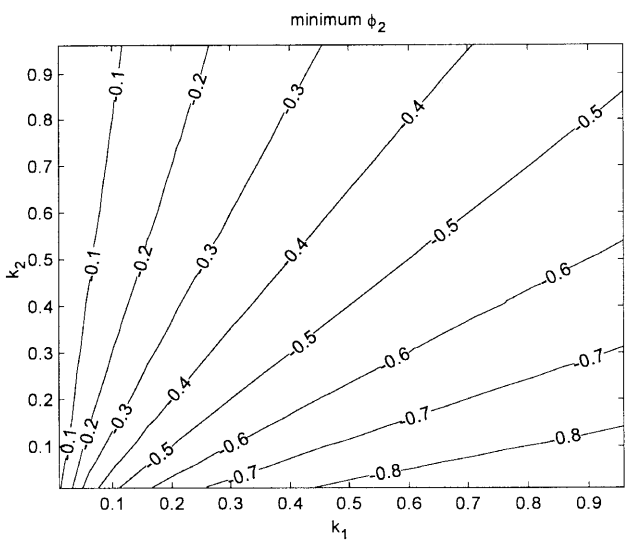

Fig. 4 Contour plot for φ_2

But at $\mathbf{h} = (0,1)^T$,

$$\mathbf{h}^T(\nabla^2\varphi_2)\mathbf{h} = -\frac{2k_1h_2^2}{(k_1+k_2+k_s)^3} < 0\,.$$

Since $\nabla^2\varphi_2$ is not positive for every $\mathbf{h} \in \mathrm{Re}^n$, Lemma 3 is not satisfied. Thus, φ_2 is proven nonconvex and Proposition 3 is proven.

Let us restrict the design variables such that $k_1, k_2 \in (0,1]$, and set $P = 1$, $k_s = 0.1$. Contours of φ_1 and φ_2 are plotted in Figs. 3 and 4. For maximum MA, optimum point is on the axis of k_1, i.e. $(k_1, 0)$. For maximum GA, optimum point is at right-lower corner, i.e. $(1, 0)$. Hence, at optimum point we see that the ground structure degenerates to a truss connecting input and output ports.

3.2 Example 2

Since the example of Sect. 3.1 is too simple to depict any practical mechanism, another example is used to illustrate the nonconvexity of the objective functions for (7) and (8). This example consists of a ground structure of six-member trusses. Five of the trusses have a length of ℓ while one of them has a length of $\sqrt{3}\ell$. The areas of the ground structure are defined by two variables, namely, A_1 and A_2. The ground structure has three degrees of freedom but only input and output displacements are of concern. The location and the direction of input and output displacements are shown in Fig. 5. As the spring model is employed, an additional spring is attached at the output port. Consequently, we have six trusses of variable cross-sectional area and a spring of fixed stiffness.

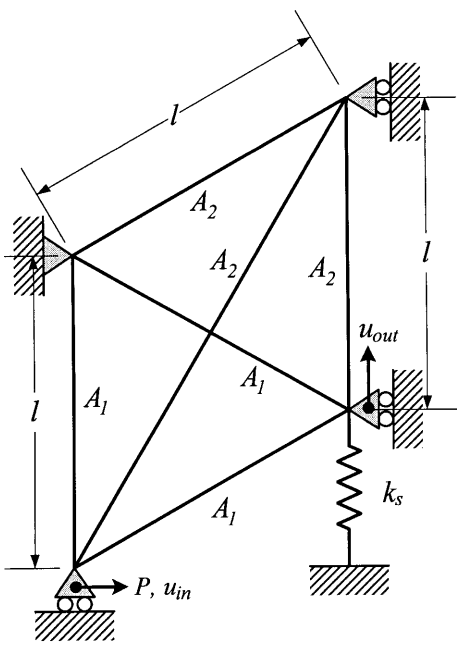

Fig. 5 Ground structure for example 2

Performing structural analysis for the discrete structure, the input and output displacements are derived analytically as below,

$$u_{\mathrm{in}} = P\frac{a_1k_1 + a_2k_2 + a_3}{b_1k_1 + b_2k_2 + b_3k_1^2 + b_4k_1k_2 + b_5k_2^2}\,, \tag{35}$$

$$u_{\mathrm{out}} = -P\frac{c_1k_1 + c_2k_2}{b_1k_1 + b_2k_2 + b_3k_1^2 + b_4k_1k_2 + b_5k_2^2}\,, \tag{36}$$

where $k_1 = A_1E/\ell$, $k_2 = A_2E/\ell$, a_i, b_j, c_n are real constants simplified from finite element analysis for $i \in \{1,2,3\}$, $j \in \{1,2,3,4,5\}$, $n \in \{1,2\}$ and are given as follows:

$$a_1 = 8.415\times10^{-1},\ a_2 = 6.830\times10^{-1},\ a_3 = 1.683\times10^{-1},$$

$$b_1 = 1.262\times10^{-1},\ b_2 = 1.804\times10^{-2},\ b_3 = 3.156\times10^{-1},$$

$$b_4 = 3.860\times10^{-1}, \quad b_5 = 3.608\times10^{-2},$$

$$c_1 = -7.288\times10^{-1}, \quad c_2 = -2.500\times10^{-1}.$$

Hence,

$$MA = \frac{k_su_{\mathrm{out}}}{P} = -\frac{k_s(c_1k_1 + c_2k_2)}{b_1k_1 + b_2k_2 + b_3k_1^2 + b_4k_1k_2 + b_5k_2^2}\,, \tag{37}$$

$$GA = \frac{u_{\mathrm{out}}}{u_{\mathrm{in}}} = -\frac{c_1k_1 + c_2k_2}{a_1k_1 + a_2k_2 + a_3}\,. \tag{38}$$

To check the convexity of the objective functions φ_1 and φ_2, mathematical manipulations similar to example 1 can be performed. In this example, it is observed that both the input and output displacements, u_{in} and u_{out}, have linear numerators but quadratic denominators with respect to design variables k_1 and k_2. Hence, the objective function φ_1, which is proportional to u_{out}, is also a function having a linear numerator and a quadratic denominator with respect to the design variables. However, it is noted that the objective function φ_2 is a ratio of two linear functions of k_1 and k_2. Hessian matrices of φ_1 and φ_2 for this example can be derived easily but they do not appear as neat as those in example 1. They can be shown to be nonconvex by substituting numerical values into their respective quadratic forms. Assume $P = 1$, $k_s = 0.1$, and the Hessian matrices of φ_1 and φ_2 at $k_1 = 0.01$ and $k_2 = 0.01$ are as follows:

$$\nabla\varphi_1 = 10^4 \times \begin{bmatrix} -1.5296 & 0.6319 \\ 0.6319 & 0.2353 \end{bmatrix}\,, \tag{39}$$

$$\nabla\varphi_2 = \begin{bmatrix} 34.1651 & 19.2000 \\ 19.2000 & 8.6601 \end{bmatrix}\,. \tag{40}$$

At $\mathbf{h} = (1, 0)^T$,

$$\mathbf{h}^T(\nabla^2\varphi_1)\mathbf{h} = -1.5296 \times 10^4 < 0\,.$$

But at $\mathbf{h} = (0, 1)^T$,

$$\mathbf{h}^T(\nabla^2\varphi_2)\mathbf{h} = 2.3531 \times 10^3 > 0\,.$$

Hence, it follows from Lemma 3 that φ_1 is nonconvex.

Similarly, φ_2 can be shown to be nonconvex because at $\mathbf{h} = (1, 0)^T$,

$$\mathbf{h}^T(\nabla^2\varphi_1)\mathbf{h} = 34.1651 > 0\,,$$

but at $\mathbf{h} = (0.5, -1)^T$,

$$\mathbf{h}^T(\nabla^2\varphi_1)\mathbf{h} = -1.9986 < 0\,.$$

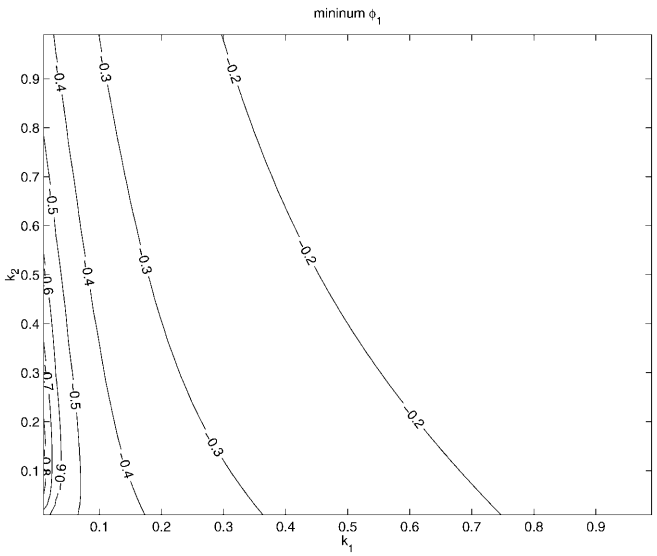

Fig. 6 Contour plot for φ_1 for Example 2

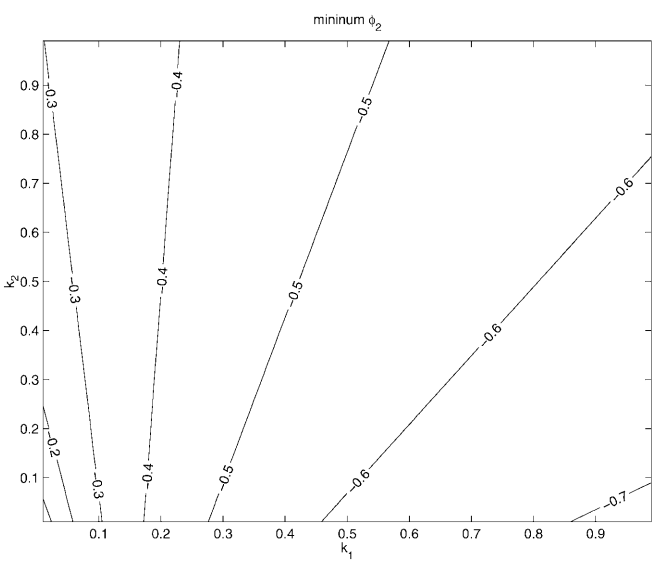

Fig. 7 Contour plot for φ_2 for Example 2

To confirm the nonconvexity, visual inspection based on contour plot and line plot can be very useful in two-dimensional problems. Let us restrict the design variables such that $k_1, k_2 \in (0, 1]$. The contour of φ_1 and φ_2 are plotted in Figs. 6 and 7. Having a sectional view on φ_1 as shown in Fig. 8, it is noticed that the curve φ_1 at $k_1 = 0.01$ is nonconvex. On the other hand, the similarity between the contour plot of φ_2 in this example and that in example 1 reveals that here φ_2 is also nonconvex.

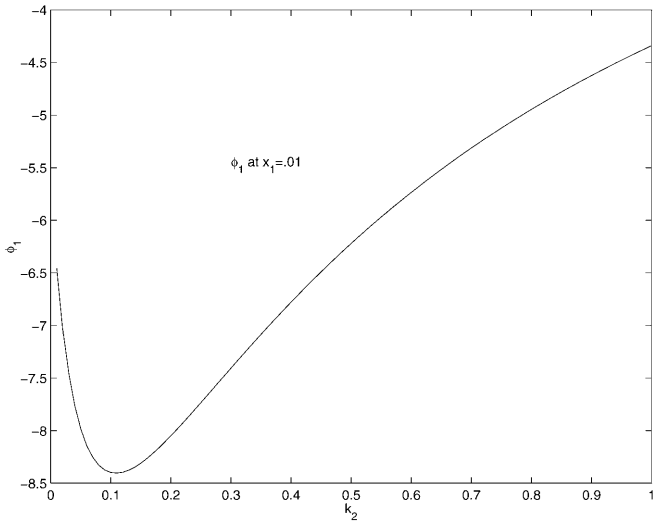

Fig. 8 Curve for φ_1 at $k_1 = 0.01$ for Example 2

For maximum mechanical advantage, or minimum φ_1, it is noticed that the optimum point is located near the point (0, 0.1). The optimum topology for maximum mechanical advantage is achieved by having a slender member defined by area A_2 as shown in Fig. 9. For

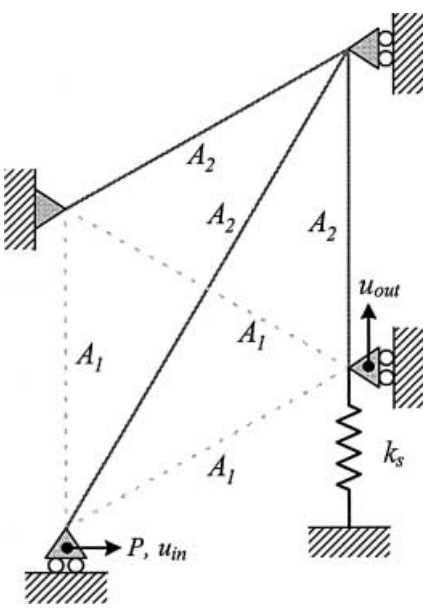

Fig. 9 Optimum topology for maximum MA

maximum geometrical advantage, or minimum φ_2, the optimum point is located at the right-lower corner, i.e. (1,0). Hence, the optimum topology for maximum geometrical advantage as shown in Fig. 10 are trusses connected in triangular shape, which can better restrain the input movement than optimum topology for maximum mechanical advantage. From the two examples above, it is concluded that propositions 2 and 3 are justified.

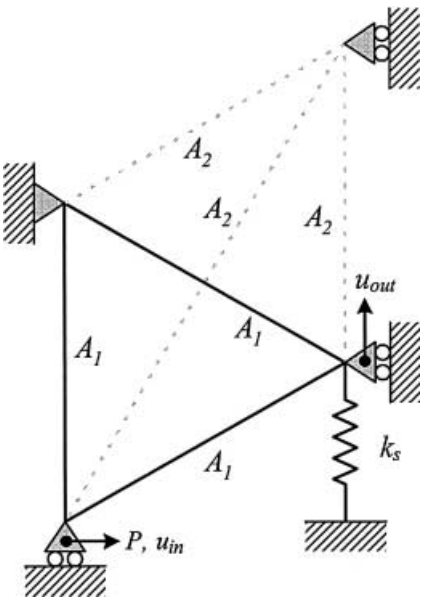

Fig. 10 Optimum topology for maximum GA

4 Effects of starting point

It has been proven that (7) and (8) are subject to convex constraints and may have nonconvex objective functions. For multivariate problems, the nonconvexity of (7) and (8) can hardly be shown analytically as in previous examples. However, if a unique solution can be obtained from a different starting point using numerical search techniques, the convexity of the problem may be assured. This is because if the problem is convex, a global optimum solution exists and can often be reached by mathematical programming regardless of the starting point. However, if the problem were nonconvex, multimodal solutions may be possible. Thus mathematical programming may not lead to a unique solution.

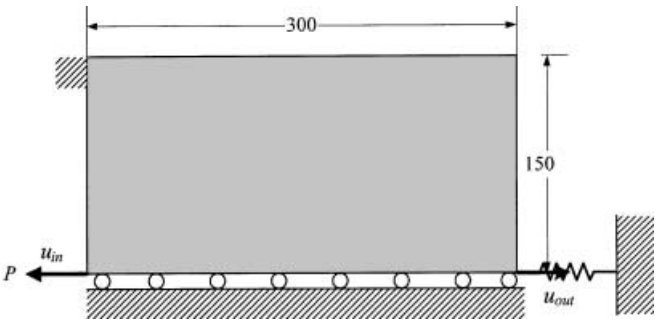

Fig. 11 Design domain for example 3

4.1 Example 3

Based on the reasoning above, (7) and (8) can be shown to be nonconvex by using the example of a displacement inverter with eight hundred design variables. As shown in Fig. 11, the design domain for the displacement inverter consists of eight hundred bilinear quadrilateral elements, which are assumed to be two-dimensional and in plane stress. The thickness, t_i, of each element is treated as a design variable. Given a horizontal input force at the left-bottom corner, the mechanical and geometrical advantages of the output port at the right-bottom corner are to be maximized separately for (7) and (8).

It is assumed that the design domain consists of a material of a Young's modulus of 200×10^3 N/mm^2, and a Poisson's ratio of 0.3. For the workpiece, a spring constant is assigned at a value of 100 N/mm. The boundary is fixed at the upper left corner while it is constrained in the y-direction at the lower bound. At the input port, a force of 100 N is imposed horizontally leftwards.

The solutions of both problem formulations are obtained using the method of moving asymptotes (Svanberg 1987), which is a method of sequential convex programming. Despite starting from two different sets of initial thickness, the solutions converge within thirty iterations. For the first set, the initial thickness is assumed to be uniformly distributed at a value of 0.3. For the second set, the initial thickness is assumed to be randomly distributed at values ranging between 0 and 1. As shown in Table 1, is observed that different initial points may lead to different optimum solutions.

The topologies for maximum mechanical advantage and their convergence histories are shown in Fig. 12. The topologies of the mechanism are shown as density contour plots. It is observed that uniformly-started optimum

Table 1 Optimum results obtained from different starting points

Starting point	Optimum $\varphi_1 = -MA$	Optimum $\varphi_2 = -GA$
uniformly distributed	-1.91583×10^{-2}	-6.86853×10^{-1}
randomly distributed	-1.87648×10^{-2}	-7.09277×10^{-1}

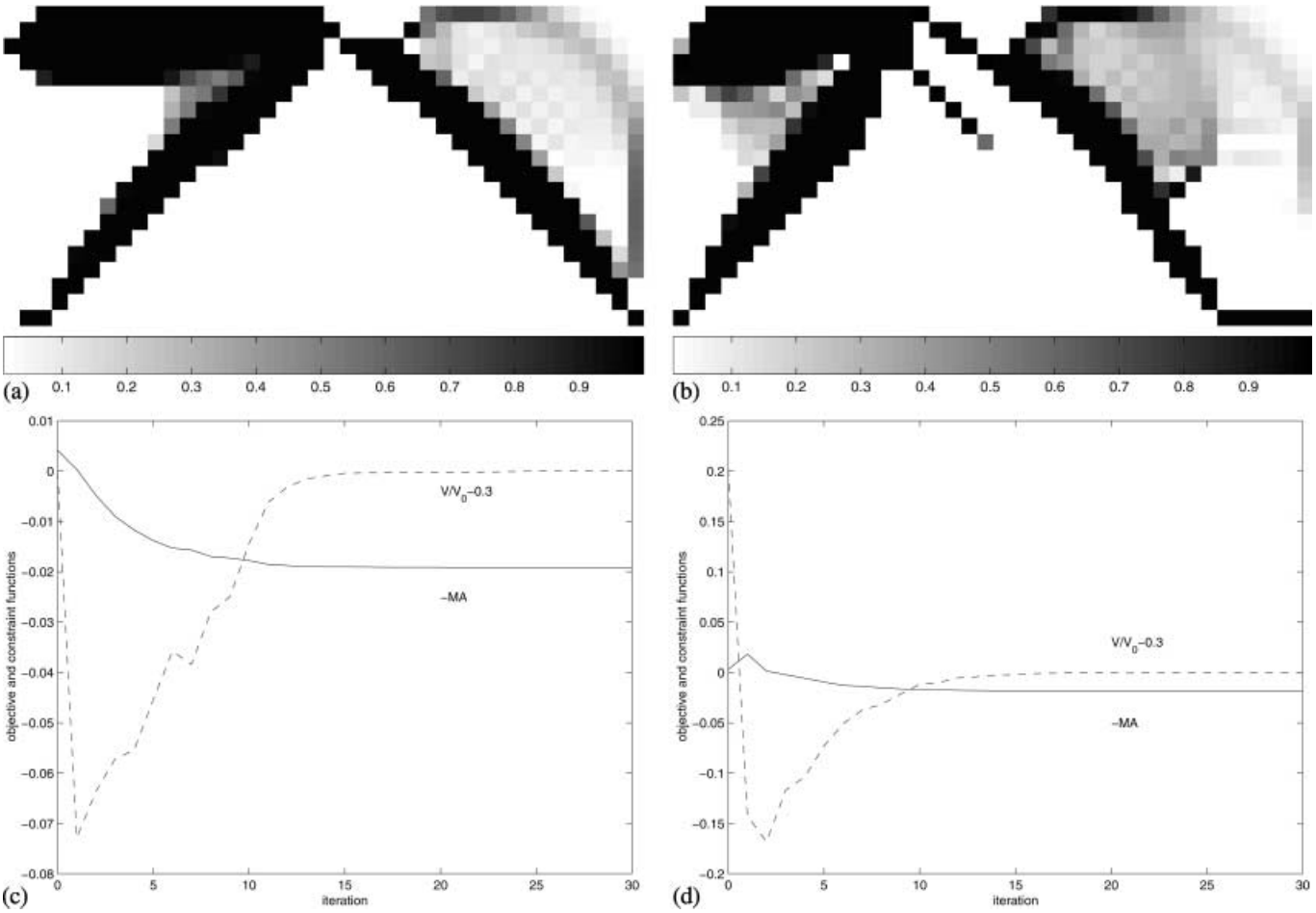

Fig. 12 (a) Topology for minimum φ_1 (uniformly started); (b) topology for minimum φ_1 (randomly started); (c) convergence history for minimum φ_1 (uniformly started); (d) convergence history for minimum φ_1 (randomly started)

topology has a longer and straighter frontal link than the randomly-started optimum topology has. Also, the former has a thinner connection between the top link and the wall. As the input displacement constraint is not violated, it is not plotted in the convergence history in Fig. 12. On the other hand, for maximum geometrical advantage, the optimum topologies and their convergence histories are shown in Fig. 13. It is observed that a randomly-started optimum topology has a thicker and straighter rear link than the uniformly-started optimum topology. Also, it is noted that the former has a smaller patch of intermediate density than the latter. As a result of lesser intermediate density, most materials are concentrated and thus they result in thicker top and rear links in the randomly-started optimum topology.

In both problems of maximum mechanical and geometrical advantages, it is observed that the major components of the optimum topologies are configured in similar connectivity although different starting points are assumed. The similarity between the topologies is especially obvious for the formulation of maximum geometrical advantage. They have the same number of major links and nearly the same location of flexural joints, which appear in the form of single-point connection between two solid elements. However, the similarity may be dependent on the problem and objective function used. For the formulation of maximum mechanical advantage, different minor components are found in the uniformly-started and the randomly-started optimum topologies. As shown in Figs. 12a and b, the latter has a residual link located between the frontal and the rear links but the former does not.

Despite similar connectivity among the major links, different sizes and shapes are generally observed among the optimum topologies, whose design variables are started uniformly or randomly. Hence, from the perspective of optimization, it is concluded that the starting point does influence the optimum topologies, and the optimization problems do not have unique solutions. Again, this example shows that (7) and (8) are nonconvex.

5 Conclusions

Based on the assumption that stiffness is linearly dependent on design variables, it is proven that problem formulations for maximum mechanical or geometrical advan-

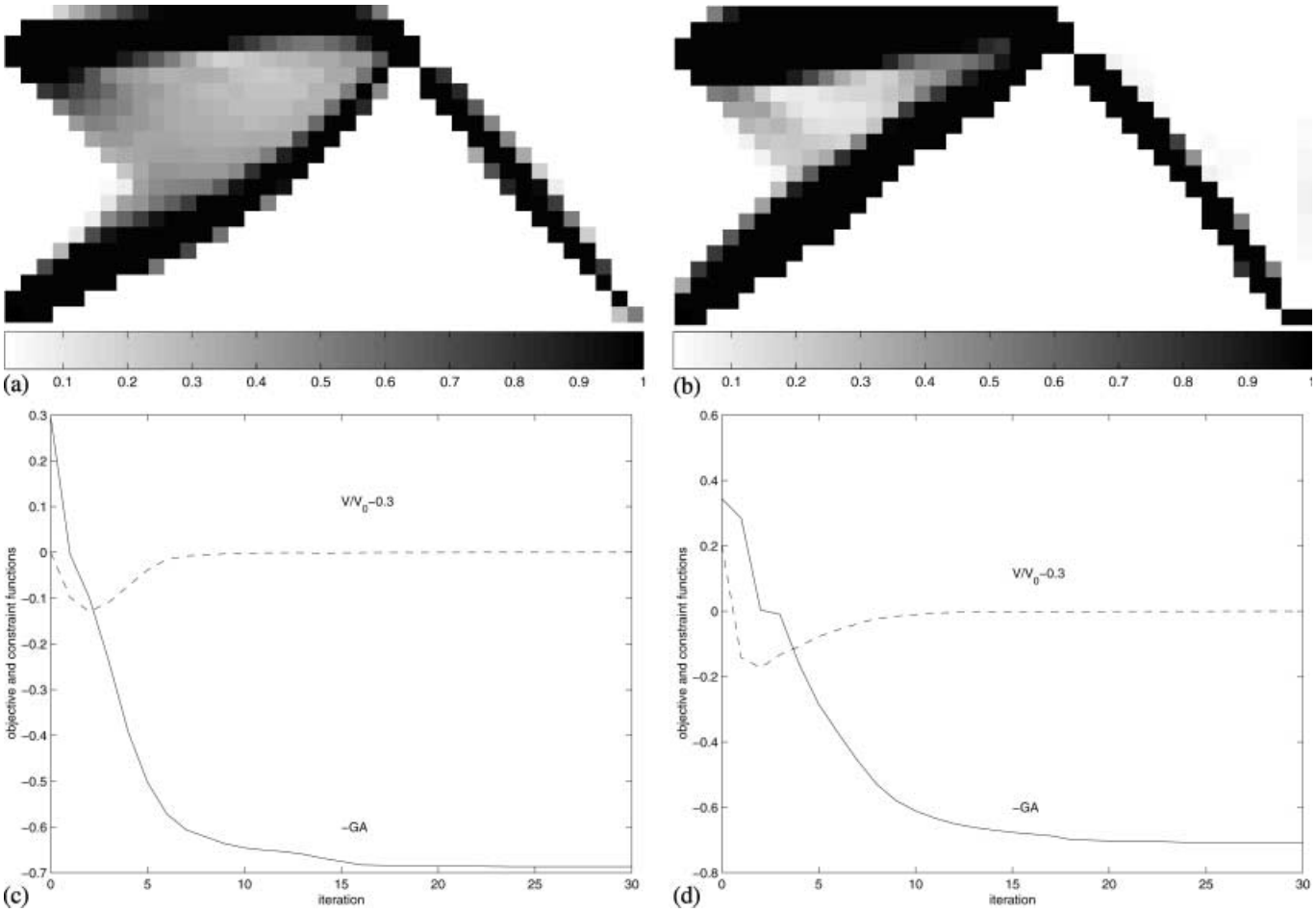

Fig. 13 (a) Topology for minimum φ_2 (uniformly started); (b) topology for minimum φ_2 (randomly started); (c) convergence history for minimum φ_2 (uniformly started); (d) convergence history for minimum φ_2 (randomly started)

tage may have nonconvex objective functions although they are subject to convex constraints. The nonconvexity of the problem formulation for compliant mechanisms is illustrated with three examples, using both the ground structure of a truss and a plane-stress membrane. If one adopts a more complex design parametrization that results in nonlinear stiffness with respect to the design variables, the problem of compliant mechanism design is expected to be complicated. In addition to the large number of design variables, the nonconvex formulation of the compliant mechanism problem may directly attribute to the higher difficulty in obtaining a feasible solution. Hence, the solution of the problem requires robust and reliable optimization techniques.

In topology optimization of compliant mechanisms, hundreds and thousands of design variables are required to represent fine topological geometry using the raster-like image of density. Hence, the topological problem can only be successfully solved if efficient, large-scale, nonconvex mathematical programming is used. Although nonconvex programming, or the stochastic optimization algorithm have been studied intensively by applied mathematicians, efficient and reliable large-scale nonconvex algorithms have yet to become available. Hence, it is recommended to resort to efficient convex approximation, which can handle large numbers of design variables. If the global optimum solution is desired, the optimization problem can be started from distinct initial points and the best result will be chosen.

Acknowledgements The authors are grateful to Krister Svanberg for providing the MMA-optimization subroutines to G.K. Lau. Also, Dr. Sun Jie from National University of Singapore is very much appreciated for his useful remarks on the proof.

References

Ananthasuresh, G.K. 1994: *A new design paradigm for micro-electro-mechanical systems and investigations on the compliant mechanism synthesis.* Ph.D. Thesis, University of Michigan, Ann Arbor, MI

Ananthasuresh, G.K.; Kota, S.; Kikuchi, N. 1994: Strategies for systematic synthesis of compliant MEMS. *Proc. ASME 1994 Winter Annual Meeting* (held in Chicago, IL). DSC-Vol. **55–2**, pp. 677–686

Bendsøe, M.P. 1989: Optimal shape design as a material distribution problem. *Struct. Optim.* **1**, 193–202

Bertsekas, D.P. 1995: *Nonlinear programming*. Athena Scientific

Frecker, M.I.; Ananthasuresh, G.K.; Nishiwaki, S.; Kikuchi, N.; Kota, S. 1997: Topological synthesis of compliant mechanism using multi-criteria optimization. *J. Mech. Des.* **119**, 238–245

Frecker, M.; Kikuchi, N.; Kota, S. 1999: Topology optimization of compliant mechanisms with multiple outputs. *Struct. Optim.* **17**, 269–278

Larsen, U.D.; Sigmund, O.; Bouwstra, S. 1997: Design and fabrication of compliant micromechanisms and structures with negative Poisson's ratio. *J. Microelectromech. Sys.* **6**, 99–106

Lau, G.K.; Du, H.; Lim, M.K. 1999: Use of functional specifications as objective functions in topological optimization of compliant mechanism. Submitted for publication

Nishiwaki, S.; Frecker, M.I.; Min S; Kikuchi, N. 1998: Topology optimization of compliant mechanisms using the homogenization method. *Int. J. Numer. Meth. Engr.* **42**, 535–559

Saxena, A.; Ananthasuresh, G.K. 1998: Topological synthesis of compliant mechanisms using the optimality criteria method. *Proc. 7th AIAA/USAF/NASA/ISSMO Symp. on Multidisciplinary Analysis and Optimization* (held in St. Louis, MO). *AIAA*, 98–4953

Sigmund, O. 1997: On the design of compliant mechanisms using topology optimization. *Mech. Struct. Mach.* **25**, 493–524

Sigmund, O. 1998: Topology optimization in multiphysics problems. *Proc. Seventh AIAA/USAF/NASA/ISSMO Symp. on Multidisciplinary Analysis and Optimization* (held in St. Louis, MO). *AIAA*, 98–4905

Svanberg, K. 1984: On local and global minima in structural optimization. In: Atrek, A.; Gallagher, R.H.; Ragsdell, K.M.; Zienkiewicz, O.C. (eds.) *New directions in optimum structural design*, pp. 327–340. New York: John Wiley and Sons

Svanberg, K. 1987: The method of moving asymptotes – a new method for structural optimization. *Int. J. Numer. Meth. Engrg.* **24**, 359–373